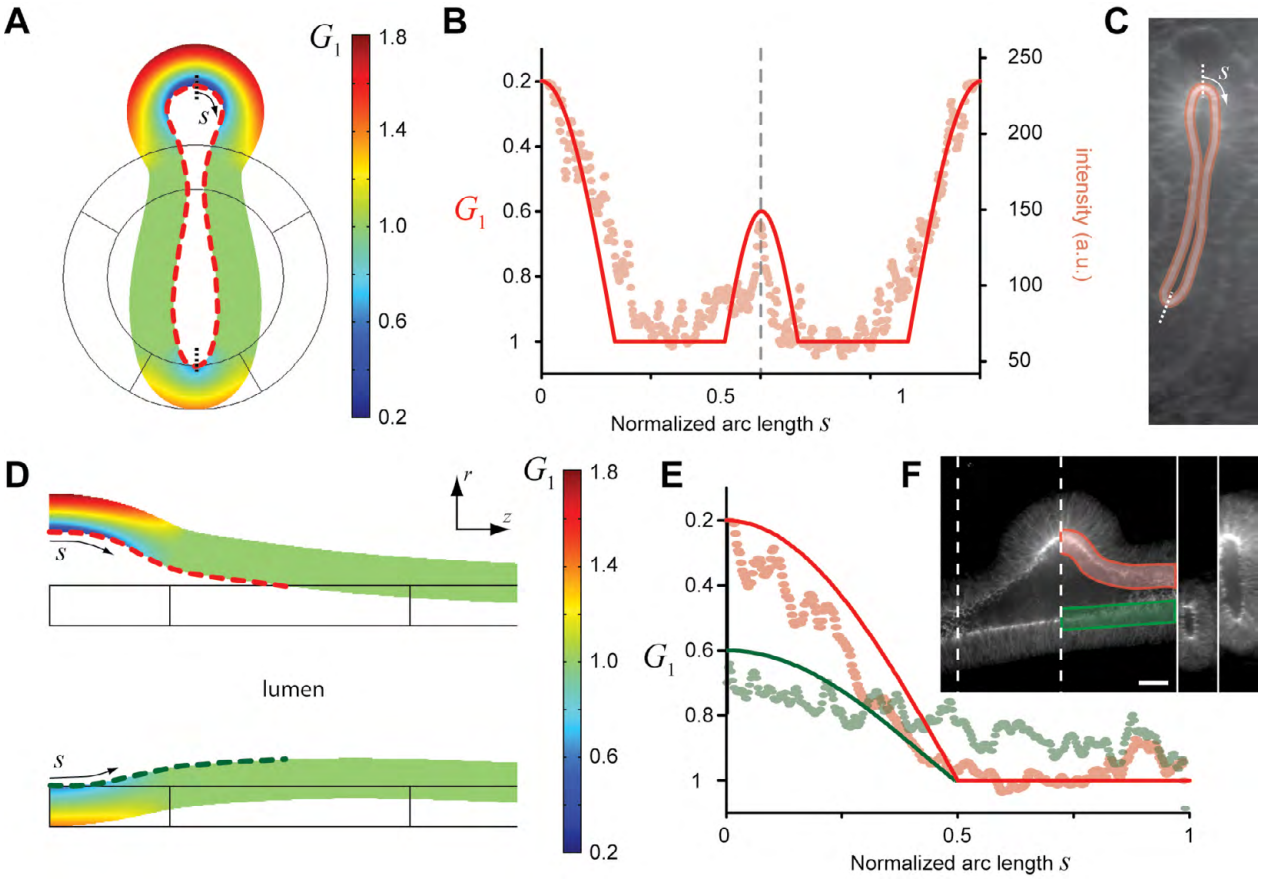

Fig. S1. Patterns of specified apical constriction based on quantitative imaging. (**A**) Transverse section of model bud geometry including only apical constriction. Surface plot of G_1 indicates regions of apical constriction; $G_1 < 1$ represents active shortening and $G_1 > 1$ represents active lengthening. (**B**,**C**) Fluorescence intensity of F-actin (red dots in B) plotted as a function of the normalized arc length *s* around the apical surface of the tube. In the model, G_1 was specified along the inner surface of the tube (dashed red line in A) in a pattern consistent with that observed experimentally (red line in B). (**D**) Longitudinal section of model bud geometry including only apical constriction. Surface plot of G_1 indicates regions of apical constriction. (**E**,**F**) Fluorescence intensity of LCAM staining along dorsal (red dots) and ventral (green dots) aspects of epithelium in 1-bud stage lung (E) and cross-sectional view of non-budding region (outlined in green) and budding region (outlined in red) (F). Scale bar: 25 μm. In the model, G_1 was specified along the dorsal and ventral surfaces of the tube (indicated by red and green lines in E) in a pattern similar to that observed experimentally.

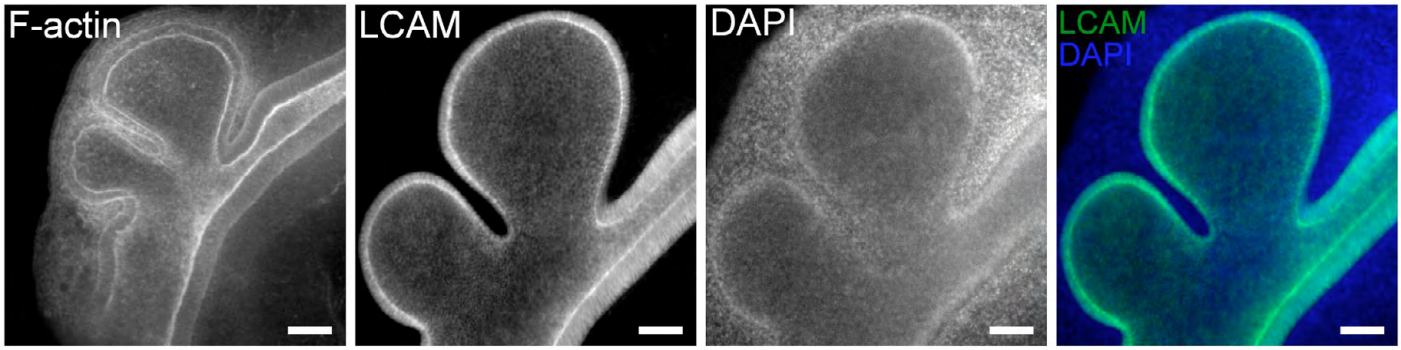

Fig. S2. Inhibiting FGFR blocks apical constriction. SU5402-treated (5 μM) lungs stained for F-actin, LCAM and DAPI. Scale bars: 50 μm.

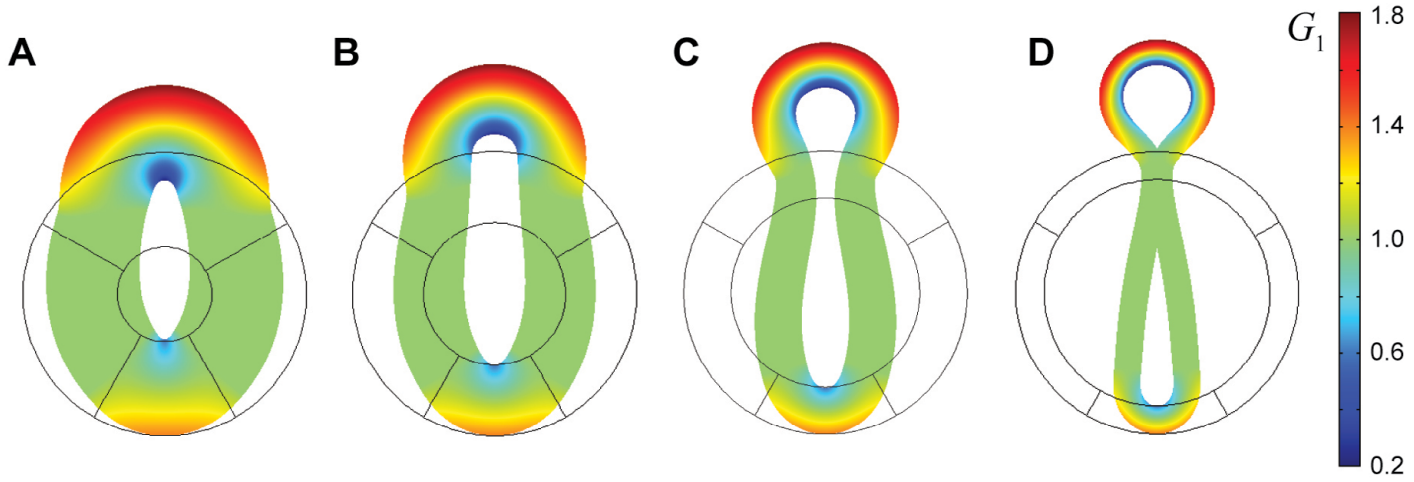

Fig. S3. Varying model tube thickness. (**A-D**) For a given increase in stiffness, the effect of apical constriction and its ability to generate a lemniscate cross-sectional geometry attenuated with increasing tube thickness.

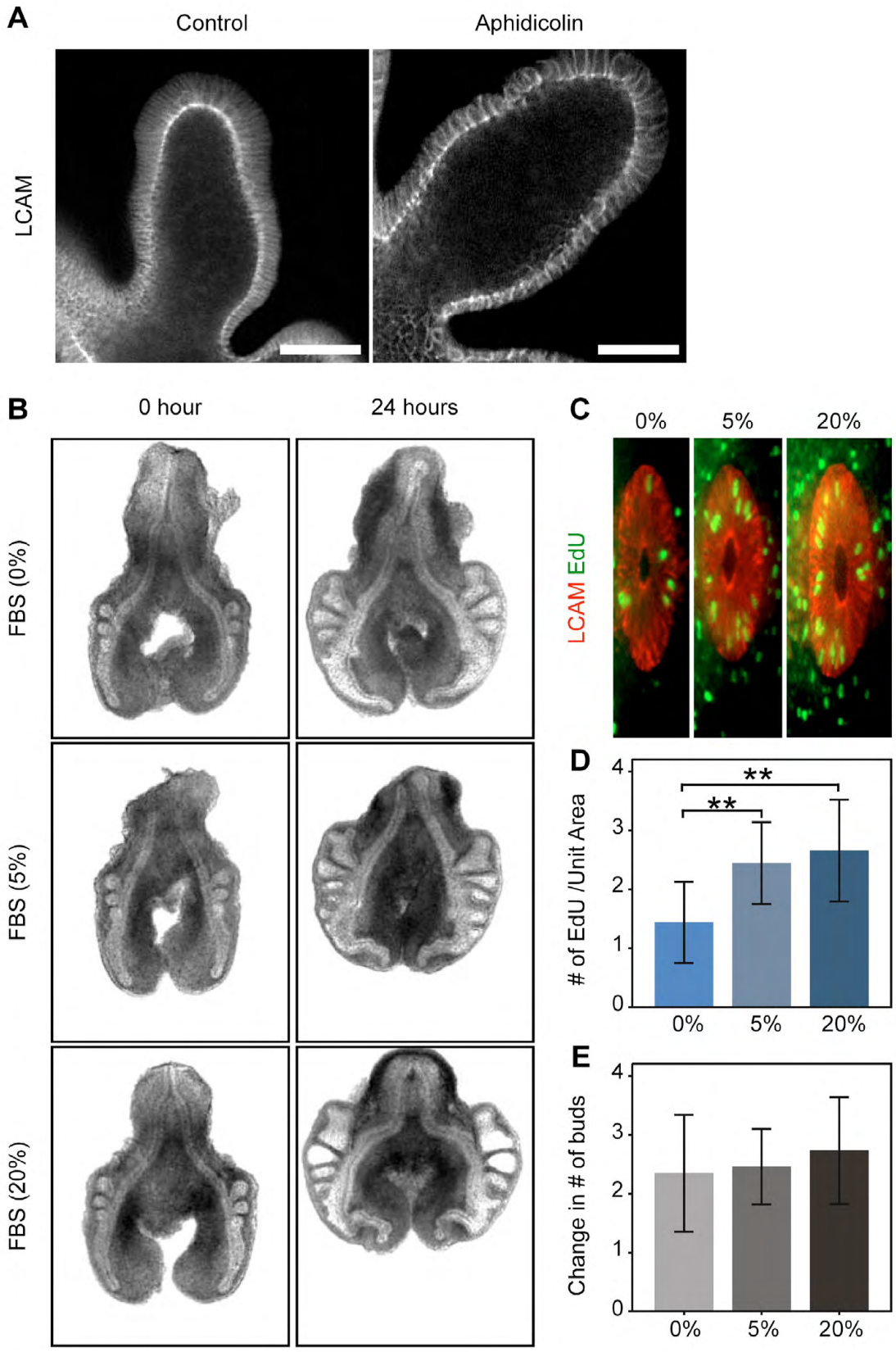

Fig. S4. Altering proliferation has no effect on budding. (**A**) High magnification of LCAM-stained lung explant from white inset in Fig. 4A. Epithelial cells are considerably larger in aphidicolin-treated airway than in control. Scale bars: 50 μm. (**B**) Brightfield images of explants cultured in different concentrations of FBS (0-20%). (**C**) Representative cross-sections of proximal regions of the lungs stained for LCAM and EdU. (**D**) Quantification of proliferating cells within proximal regions of epithelium in different concentrations of FBS (0-20%) (unit area=400 μm^2, n>4, $^{**}P$<0.01, error bars represent s.d.). (**E**) Change in the number of buds after 24 hours of culture in FBS (0-20%). (n>12, error bars represent s.d.).

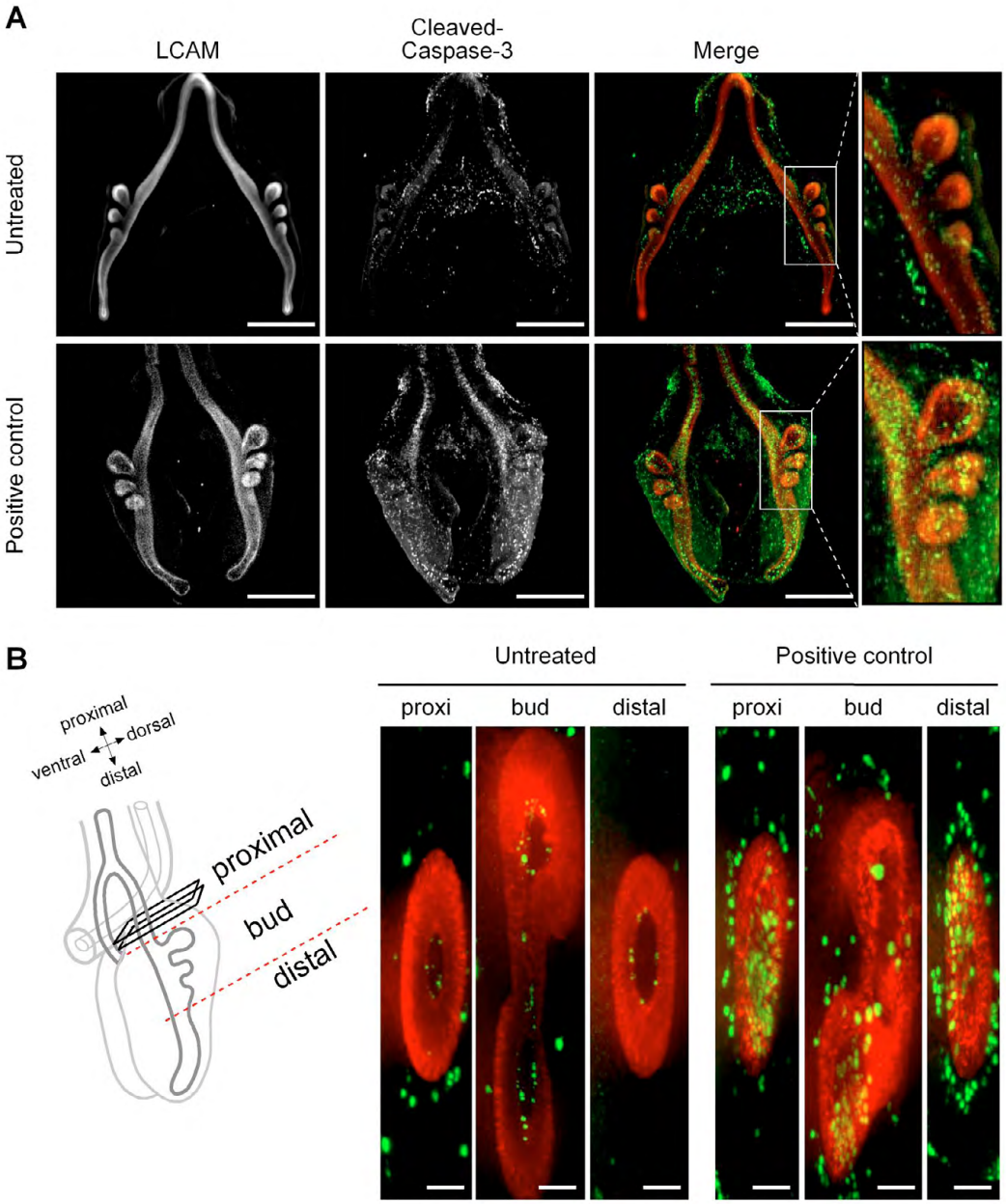

Fig. S5. The airway epithelium is essentially non-apoptotic during monopodial budding. (**A**) Representative lung explants stained for LCAM and cleaved caspase-3 show few apoptotic cells in the airway epithelium. Scale bars: 500 μm. (**B**) Maximum intensity of 30 μm-thick tissue cross-sections along the primary bronchus. Scale bars: 100 μm. Positive controls were treated with staurosporine (1 μM) for 3 hours.

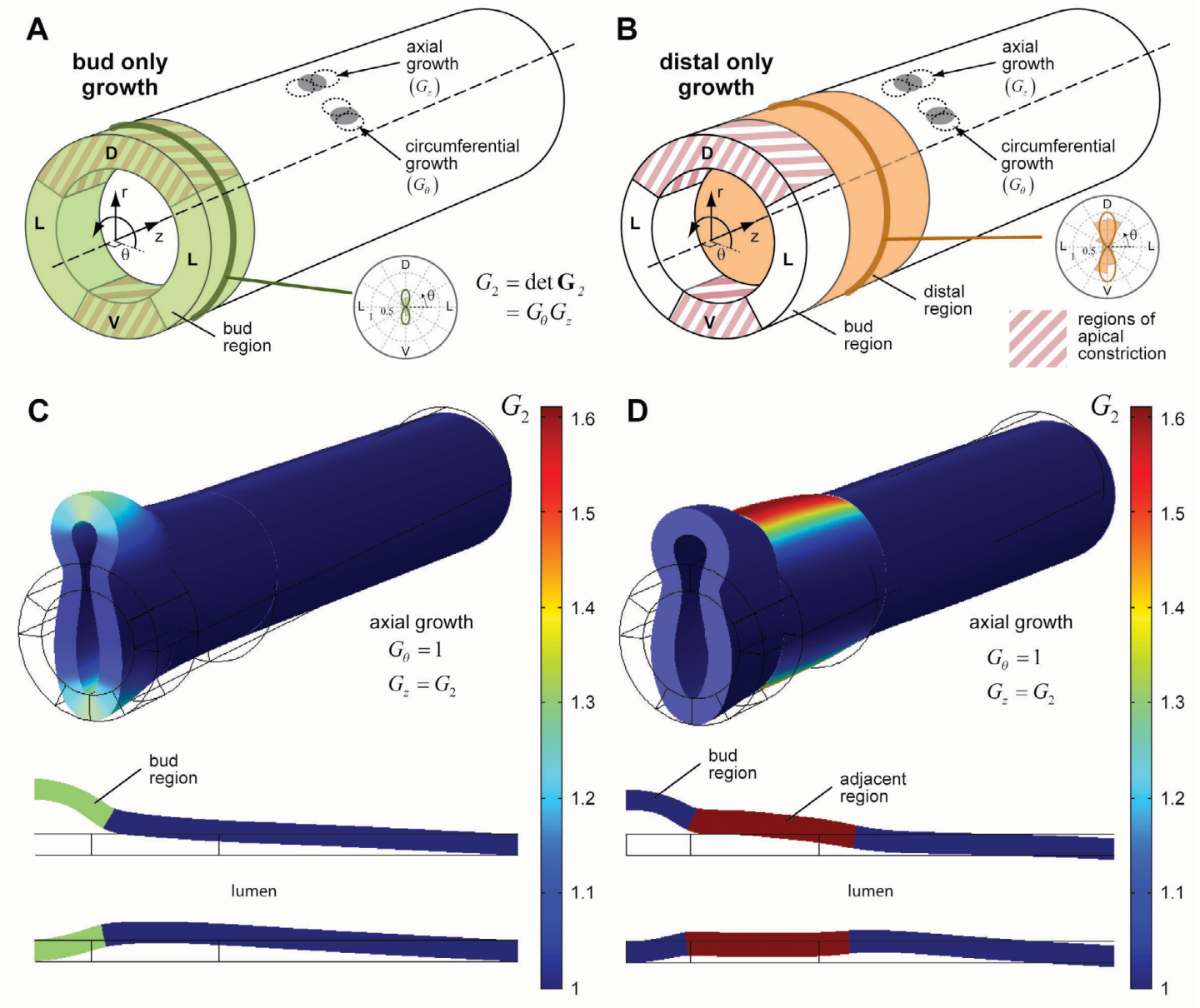

Fig. S6. Proliferation is necessary in both bud and distal regions to form neck-like region. (**A**,**B**) Model schematics. Axial proliferation was specified in the (A) bud or (B) distal region of the tube alone. (**C**,**D**) Deformed geometry of both models indicates that neither is able to generate a neck-like region in the bud.

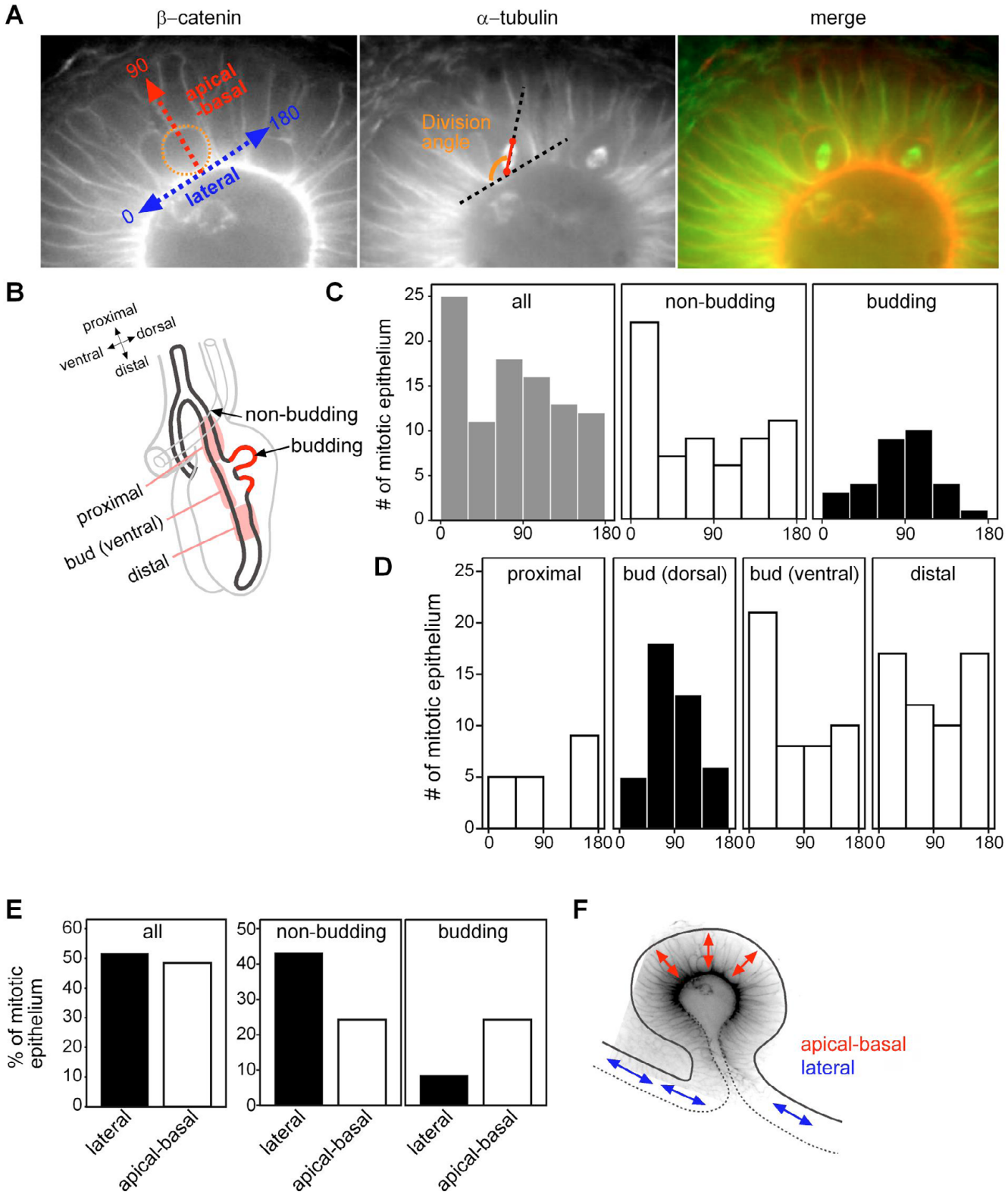

Fig. S7. Analysis of division angles within the epithelium of the primary bronchus during monopodial budding. (**A**) Embryonic chicken lung stained for β-catenin and α-tubulin. Division angles were measured in reference to the axes of the epithelium [apical-basal (90°) and lateral (0-180°) axes of the epithelial cell]. (**B**) Schematic of the embryonic chicken lung shows the regions specified in C-E. (**C-E**) Quantification of angles of the mitotic spindle during and after anaphase. (*n*=95 from five lungs). Percentage of mitotic epithelium in apical-basal direction (45-135°) and lateral direction (0-45° and 135-180°) shown in E. (**F**) Schematic shows the preferential direction of division angles within the budding epithelium.

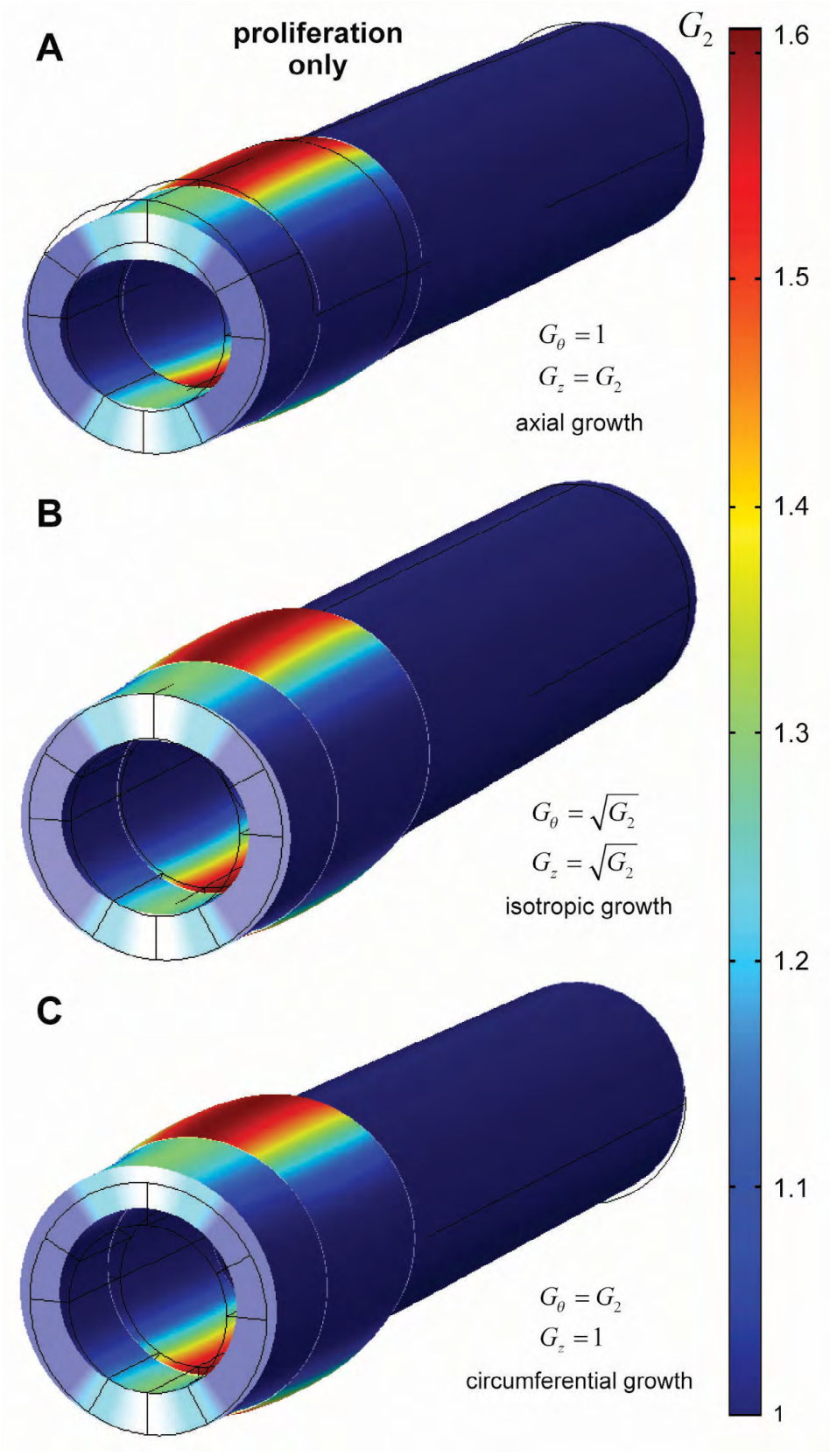

Fig. S8. Cell proliferation alone does not produce a lung bud. (**A-C**) Without changing any other parameters, we removed apical constriction from the model (and thereby also any tissue stiffening) and considered the effects of proliferation alone. 3D deformed model geometry for (A) axial growth, (B) isotropic growth and (C) circumferential growth. In each case, the model failed to produce a bud.

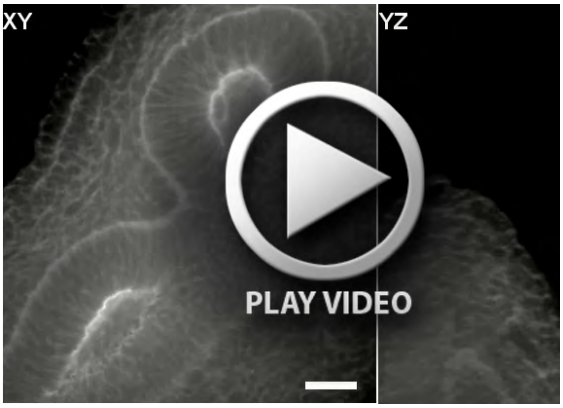

Movie 1. Confocal stack of F-actin-stained embryonic chicken lung. White lines in *xy* panel show the positions that projected in *yz* panel. Still images are shown in Fig. 2A. Scale bar: 20 μm.

Movie 2. 3D deformed shape of model including only apical constriction. $G_1 < 1$ indicates active shortening, whereas $G_1 > 1$ indicates lengthening. Scale factor=1. Final frame is shown in Fig. 3B.

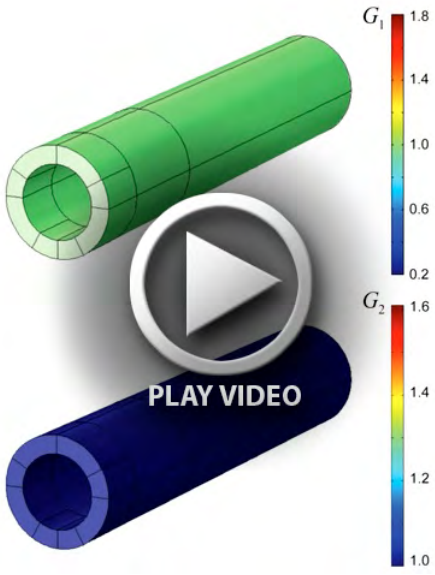

Movie 3. 3D deformed shape of model including both apical constriction and axial proliferation. At the top, a surface plot of G_1, which indicates the spatial distribution of apical constriction. $G_1 < 1$ indicates active shortening, whereas $G_1 > 1$ indicates lengthening. On the bottom, a surface plot of G_2, which specifies the overall amount of proliferation. $G_2 > 1$ represents an increase in cell proliferation. Scale factor=1.